Geophys. J. Int. (2003) **155,** 139–148

Amplitude fluctuations due to diffraction and refraction in anisotropic random media: implications for seismic scattering attenuation estimates

T. M. Müller* and S. A. Shapiro

Fachrichtung Geophysik, Freie Universität Berlin, Malteserstr. 74-100, *Haus D,* 12249 *Berlin, Germany. E-mail: tmueller@geophysik.fu-berlin.de*

Accepted 2003 April 30. Received 2003 April 23; in original form 2002 April 22

SUMMARY

We calculate the variance of the log-amplitude within the Rytov approximation for plane waves propagating in weakly inhomogeneous and statistically anisotropic random media. Since there is a simple relation between the log-amplitude variance and the attenuation coefficient of seismic primaries in the weak wavefield fluctuation regime, we also obtain scattering attenuation estimates that additionally depend on the aspect ratio of longitudinal and transverse correlation scales of the inhomogeneities. These estimates can be useful for the statistical characterization of anisotropic, large-scale inhomogeneities (large compared with the wavelength of the probing pulse) in the Earth crust and mantle, such as fault zones. With the help of plane-wave-transmission numerical experiments using the finite-difference method we compute the log-amplitude variance as a function of the propagation distance and observe reasonable agreement with the analytical results. We discuss the implications of our results in the context of seismic scattering attenuation estimations.

Key words: anisotropic random media, crustal heterogeneities, diffraction, refraction, scattering attenuation, seismic primaries.

1 INTRODUCTION

In seismology it is common practice to analyse the amplitude and phase fluctuations of transmitted and reflected seismic signals in order to statistically characterize the subsurface heterogeneities. In particular, the Rytov approximation for the variance of the log-amplitude and phase fluctuations of diffracted and refracted waves has been applied in several studies (Wu & Flatté 1990; Sato & Fehler 1998, and references therein; Tripathi 2001). For example, Wu & Flatté (1990) derived from seismograms of the NORSAR array the log-amplitude and phase (and their cross-) correlation function and modelled them with the corresponding correlation functions for isotropic random media. It is well known that the diffraction and refraction of waves at *randomly* distributed inhomogeneities results in a random focusing and defocusing of wave energy and consequently results in an increase of the amplitude fluctuations with increasing propagation distances (Rytov *et al.* 1989). Diffraction of seismic waves becomes noticeable if the size of an inhomogeneity exceeds the wavelength. A measure that distinguishes the importance of diffraction and refraction effects is the wave parameter D, which is defined as the ratio of the size of the Fresnel zone and the characteristic length-scale of the inhomogeneities (if $D \ll 1$ refraction prevails, whereas for $D \gg 1$ both, diffraction and refraction effects occur). Shapiro & Kneib (1993) showed that the variance of the log-amplitude fluctuations is directly related to the coefficient of scattering attenuation and thus to the scattering quality factor, which is another important quantity in order to characterize the propagation medium.

All of the above-mentioned works use the model of an isotropic random medium. There is, however, a lot of evidence that at some sites the heterogeneities of the crust are anisotropic. Indeed, from the analysis of well-log data at the KTB deep borehole, Wu *et al.* (1994) suggested a model of randomly distributed velocity inhomogeneities with a lateral characteristic scale of 3.6 km and a vertical scale of 2 km. Also parts of the lithospheric mantle are assumed to be composed of anisotropic heterogeneities: Ryberg *et al.* (1995) deduced from short-period wavefield data recorded on a profile across Northern Eurasia that this zone contains randomly distributed, spatially anisotropic velocity fluctuations, which are 'stretched' in the horizontal direction. Based on a modelling study of these data, Tittgemeyer *et al.* (1999) provide a generic description of lower-crust and upper-mantle heterogeneities with a ratio of anisotropy (the aspect ratio of vertical and horizontal correlation scale) of $\approx$0.25. Analysing the P-coda characteristics in seismograms from local events at the San Jacinto fault zone, Wagner (1998) concluded that a model of a grossly plane-layered structure statistically described by a spatially anisotropic correlation function would be most consistent with the observations. He raised concern about the 'overlooked

*Now at: Department of Exploration Geophysics, Curtin University of Technology, PO Box U1987, Perth, WA 6845, Australia.

alternative' to allow the heterogeneities to be spatially anisotropic. Thus, when analysing the statistical properties of wavefields recorded in such regions it is necessary to include the anisotropy of the inhomogeneities (this is also pointed out in the book of Sato & Fehler 1998). Estimates of the strength of the medium perturbations, their correlation properties and of the quality factor will be more reliable if the model of statically isotropic inhomogeneities is generalized to also allow anisotropic inhomogeneities. To the best of our knowledge, there exist no explicit results on how large-scale, anisotropic inhomogeneities affect the amplitudes of seismic primary arrivals.

Kon (1994) presented a qualitative theory of amplitude and phase fluctuations due to diffraction in anisotropic, turbulent media based on the consideration of randomly distributed, collecting and diverging lenses (the isotropic case has been previously discussed in this manner by Rytov *et al.* 1989). Kon (1994) showed that waves propagating along the short axis of inhomogeneities exhibit decreasing amplitude and phase fluctuations compared with the isotropic case. In contrast, waves propagating parallel to the long axis of the inhomogeneities show stronger fluctuations. In order to describe the statistical moments in weakly inhomogeneous media the Markov and the Rytov approximations are frequently employed (Rytov *et al.* 1989). Both approximations are restricted by the small-angle scattering (or equivalently forward-scattering) assumption. Dashen (1979) argued that the Markov approximation can fail in anisotropic random media because the scattering angles grow successively while the wave passes from one inhomogeneity to the next (this effect is most pronounced when the wave initially propagates along the long axis of the inhomogeneities see Fig. 1). It may be suspected that the same argument holds for the Rytov approximation. By solving the single-scattering problem for anisotropic heterogeneities (with the correlation scales a_x, a_y and a_z, where $a_x = a_z \gg a_y$), Beran & McCoy (1974) showed that for the case $ka_x \gg 1$ (k is the wavenumber) the scattering angles in the directions x, z and y are of the order of $\theta_{x,z} = O(1/ka_x)$ and $\theta_y = O(1/\sqrt{ka_x})$, respectively. They concluded that a more stringent condition for the validity of small-angle scattering approximations must be imposed compared with the isotropic scattering problem, where $\theta = O(1/ka)$.

In spite of the possibility of treating anisotropic inhomogeneities within the Rytov approximation, usually only final results and discussions for the isotropic case are found (e.g. Ishimaru 1978; Rytov *et al.* 1989). Exceptionally, in the works of Komissarov (1964) and Knollman (1964) the anisotropic case is investigated, resulting in rather complicated expressions for the second-order moments of the wavefield. Moreover, Knollman considers the amplitude fluctuations instead of the log-amplitude fluctuations. More recently, the variance of the phase fluctuations, which serves as a measure of the velocity shift, has been analysed in detail for anisotropic random media by Samuelides (1998). However, tractable, explicit results for the log-amplitude variance in the Rytov approximation valid for anisotropic random media are not known at present. It is the purpose of this research note to fill this gap and to discuss its significance in the context of seismic scattering attenuation. That is to say, we do not rederive the Rytov approximation, but on the basis of explicit results (which we verify numerically) we focus on its applicability in anisotropic random media.

The outline of our consideration is the following. First we briefly formulate the problem of seismic scattering in randomly inhomogeneous media within the framework of the stochastic scalar wave equation and provide the basic relations necessary for subsequent sections. Then, an expression of the log-amplitude variance using the Rytov approximation is derived. In Section 4 explicit results for Gaussian random media are presented. The frequency and travel distance dependence of the log-amplitude variance are analysed. The analytical results are verified numerically with the help of finite-difference simulations (Section 5). In Section 6 we discuss our results in the context of seismic scattering attenuation estimates. The results are also discussed in the light of previously obtained approximations for the scattering attenuation coefficient in 3-D isotropic and 1-D random media.

2 ATTENUATION DUE TO DIFFRACTION AND REFRACTION

In order to study the propagation of waves in randomly inhomogeneous media we use the acoustic wave equation

$$\Delta u(t, \mathbf{r}) - p^2(\mathbf{r}) \frac{\partial^2 u(t, \mathbf{r})}{\partial t^2} = 0, \tag{1}$$

where we have defined the squared slowness as $p^2(\mathbf{r}) = \frac{1}{c_0^2}[1 + 2n(\mathbf{r})]$, where c_0 denotes the propagation velocity in a homogeneous reference medium. The function $n(\mathbf{r})$ is a realization of a stationary random field with zero average, i.e. $\langle n(\mathbf{r}) \rangle = 0$ and is characterized by a spatial correlation function $B_n(\mathbf{r}) = \langle n(\mathbf{r}_1)\, n(\mathbf{r}_2) \rangle$, which only depends on the difference vector $\mathbf{r} = \mathbf{r}_1 - \mathbf{r}_2$. The variance of the random function n is denoted by $B_n(0) = \sigma_n^2$. A solution of eq. (1) in the form of time-harmonic wavefields can be presented using the Rytov transformation

$$u(\omega; \mathbf{r}) = A_0 e^{\Psi(\omega; \mathbf{r})}, \tag{2}$$

where the complex function Ψ is composed of the so-called log-amplitude fluctuations

$$\mathrm{Re}\{\Psi\} \equiv \chi \equiv \ln(A/A_0), \tag{3}$$

and the phase fluctuations $\mathrm{Im}\{\Psi\} \equiv \tilde{\phi} \equiv \phi - \phi_0$. Here the quantities A and ϕ denote the current amplitude and phase, respectively. The quantities A_0 and ϕ_0 define the incident wavefield $u_0 = A_0 \exp(i\phi_0)$ propagating through the homogeneous reference medium ($n(\mathbf{r})$=0).

It has been shown that the mean ($\langle \chi \rangle$) and the variance (σ_χ^2) of the log-amplitude fluctuations are related through (Rytov *et al.* 1989)

$$\langle \chi \rangle = -\sigma_\chi^2, \tag{4}$$

where the variance is defined as $\sigma_\chi^2 \equiv \langle (\chi - \langle \chi \rangle)^2 \rangle$. Eq. (4) is valid as long as the wavefield fluctuations are weak and the waves are mainly scattered in the forward direction. Such a regime exists if

$$\sigma_\chi^2 (ka)^2 \frac{L}{a} < 1 \tag{5}$$

and $ka \gtrsim 1$, where ka and L/a denote the normalized wavenumber and travel distance, respectively (normalized by the correlation length a). In order to obtain global scattering attenuation estimates, Shapiro & Kneib (1993) used the fact that the attenuation coefficient α of a plane wave can be expressed through the mean of the log-amplitude fluctuations

$$\alpha = -\frac{\langle \chi \rangle}{L} = \frac{\sigma_\chi^2}{L}. \tag{6}$$

Hence, the key to the description of attenuation due to random diffraction and refraction is the computation of the log-amplitude variance σ_χ^2. For the case of statistically isotropic random media, in the second-order Rytov approximation one obtains (Ishimaru 1978)

$$\sigma_\chi^2 = 2\pi^2 k^2 L \int_0^\infty d\kappa \kappa \Phi_n(\kappa) \left[1 - \frac{\sin(\kappa^2 L/k)}{\kappa^2 L/k} \right], \tag{7}$$

where $\Phi_n(\kappa)$ denotes the fluctuation spectrum, i.e. the 3-D Fourier transform of the correlation function B_n.

3 LOG-AMPLITUDE VARIANCE FOR ANISOTROPIC RANDOM MEDIA

In anisotropic or isotropic random media the calculation of the variance of the log-amplitude fluctuations is based on that for the transverse correlation function $B_\chi = \langle \chi \chi^\star \rangle$, because by definition $\sigma_\chi^2 \equiv B_\chi(\boldsymbol{\rho} = 0)$, where $\boldsymbol{\rho}$ denotes the spatial coordinates transverse to the direction of the incident wave (x-direction). The log-amplitude correlation function at zero lag is given by the following expression (Ishimaru 1978, eq. 17.44):

$$\sigma_\chi^2 = k^2 \int_0^L dx' \int_0^L dx'' \iint d\boldsymbol{\kappa} \times F_n(x' - x'', \boldsymbol{\kappa}) \sin\left(\frac{L - x'}{2k}\kappa^2\right) \sin\left(\frac{L - x''}{2k}\kappa^2\right), \tag{8}$$

where F_n denotes the 2-D Fourier transform of the correlation function B_n in the transverse coordinates $\boldsymbol{\rho}$,

$$F_n(x' - x'', \boldsymbol{\kappa}) = \frac{1}{4\pi^2} \iint B_n(x' - x'', \boldsymbol{\rho}) \mathrm{e}^{-i\boldsymbol{\kappa}\boldsymbol{\rho}}\, d\boldsymbol{\rho}. \tag{9}$$

Note that eqs (8) and (9) are also valid in the general case when the direction of wave propagation x does not coincide with the axes of the correlation lengths of the inhomogeneities. In this case the correlation function B_n can be transformed in order to make explicit the dependence on the angle between planes transverse to the direction of propagation and the planes spanned by the axes of the correlation lengths (see, e.g., Samuelides 1998).

In the next step, the difference and centre-of-mass coordinates $x_\mathrm{d} = x' - x''$ and $\eta = \frac{x' + x''}{2}$ are introduced and the ranges of integration are transformed according to eq. (17.46) of Ishimaru (1978): $\int_0^L dx' \int_0^L dx''\,(\cdot) \approx \int_0^L d\eta \int_{-\infty}^{\infty} dx_\mathrm{d}\,(\cdot)$. In the derivation of σ_χ^2 for the isotropic case it is assumed that the sine terms in eq. (8) are slowly varying functions of x' and x'' because $\kappa^2 a/k < 1/ka \lesssim 1$ and therefore these variables are replaced by the centre-of-mass coordinate η, i.e. $\sin(\frac{L-x'}{2k}\kappa^2)\sin(\frac{L-x''}{2k}\kappa^2) \approx \sin^2(\frac{L-\eta}{2k}\kappa^2)$. However, this replacement means that local variations of the medium parameters in the direction of wave propagation are not taken into account and consequently the correlation length in the direction of wave propagation, $a_{||}$, becomes a redundant parameter. This is admissible in isotropic random media, where it is known that the correlation length transverse to the direction of wave propagation, $a_\perp$, mainly controls the strength of the wavefield fluctuation (Ishimaru 1978, chapter 20). Considering anisotropic random media, though, more accurate results can be obtained when all terms inside the sine functions in eq. (8) are retained when introducing the centre-of-mass coordinate η. Thus, we have $\sin(\frac{L-x'}{2k}\kappa^2)\sin(\frac{L-x''}{2k}\kappa^2) = \cos^2(\frac{x_\mathrm{d}}{4k}\kappa^2) - \cos^2(\frac{L-\eta}{2k}\kappa^2)$. Performing now the integration with respect to η, eq. (8) modifies to

$$\sigma_\chi^2 = k^2 L \iint d\boldsymbol{\kappa} \int_0^\infty dx_\mathrm{d} F_n(x_\mathrm{d}, \boldsymbol{\kappa}) \times \left[\cos\left(\frac{x_\mathrm{d}}{2k}\kappa^2\right) - \frac{\sin(\kappa^2 L/k)}{\kappa^2 L/k}\right]. \tag{10}$$

This equation has a similar structure to the isotropic result (7), however, it involves an additional integration with respect to the difference coordinate x_d which cannot be performed without specifying the correlation function B_n and hence F_n. Eq. (10) together with eq. (6) provides an estimate of the scattering attenuation coefficient of seismic primaries in anisotropic random media. That is to say, eq. (10) allows one to study the behaviour of the scattering attenuation coefficient if the propagation direction and the principal axes of the inhomogeneities are at arbitrary angles to each other. Its domain of validity is examined in the next section. An analogous result for σ_χ^2 can be obtained in 2-D random media. In particular, dividing eq. (10) by π, and using the 1-D Fourier transform of B_n instead of eq. (9) yields the 2-D result for σ_χ^2. We note that the variance of the phase fluctuations, the crossvariance between log-amplitude and phase fluctuations and also the transverse correlation functions can be treated in the same manner. This is, however, not the topic of the present study.

4 EXPLICIT RESULTS FOR GAUSSIAN RANDOM MEDIA

In order to obtain explicit results from eq. (10) we have to specify the correlation function B_n. We choose a Gaussian correlation function $B_n(\mathbf{r}) = \sigma_n^2 \exp(-\frac{x^2}{a_x^2} - \frac{y^2}{a_y^2} - \frac{z^2}{a_z^2})$. Despite the fact that a Gaussian correlation function does not reflect the correlation properties of the micro- and macrostructure of real rocks (e.g. Klimeš 2002), its use is most convenient in order to compare theoretical and numerical results. However, we note that any correlation function that decreases sufficiently rapid with increasing correlation lag (so that the integrals in eq. 10 converge) could be used.

For simplicity, we consider the case of wave propagation in the x direction so that the correlation length parallel to this direction is $a_{||} = a_x$ and also assume that $a_y = a_z = a_\perp$, i.e. isotropy in the transverse plane. Then, the correlation function is of the form

$$B_n(\mathbf{r}) = \sigma_n^2 \exp\left(-\frac{x^2}{a_{||}^2} - \frac{\rho^2}{a_\perp^2}\right) \tag{11}$$

and with help of eq. (9), which in the given geometry degenerates to the Hankel transform, one obtains

$$F_n(x_\mathrm{d}, \kappa) = \sigma_n^2 \frac{a_\perp^2}{4\pi} \exp\left(-x_\mathrm{d}^2/a_{||}^2\right) \exp\left(-\kappa^2 a_\perp^2/4\right). \tag{12}$$

Inserting eq (12) into (10) and performing the integrations with respect to x_d and κ, we obtain

$$\sigma_\chi^2 = \sigma_n^2 \frac{\sqrt{\pi}}{16} k^4 a_\perp^4 \left\{\sqrt{\pi}\mathrm{e}^{1/A^2}[1 - \mathrm{erf}(1/A^2)]2D - A \arctan(2D)\right\}, \tag{13}$$

where erf denote the error function and we introduced the dimensionless quantities $D = 2L/ka_\perp^2$ (known as the wave parameter) and $A = 2\,a_{||}/ka_\perp^2$. For $ka_\perp > 1$, which is required in order to satisfy restriction (5), eq. (13) can be simplified to

$$\sigma_\chi^2 \approx \sigma_n^2 \frac{\sqrt{\pi}}{4} \frac{a_{||}}{a_\perp} k^3 a_\perp^3 D \left[1 - \frac{\arctan(2D)}{2D}\right]. \tag{14}$$

An analogous calculation yields the 2-D result

$$\sigma_\chi^2 \approx \sigma_n^2 \frac{\sqrt{\pi}}{4} \frac{a_{||}}{a_\perp} k^3 a_\perp^3 D \left(1 - \frac{1}{\sqrt{2}D}\sqrt{\sqrt{1 + 4D^2} - 1}\right). \tag{15}$$

It is interesting to note that in the case $a_{||} = a_\perp$, formulae (14) and (15) exactly coincide with the formulae of σ_n^2 for the isotropic case (e.g. Müller *et al.* 2002). Therefore, the ratio $\gamma = a_{||}/a_\perp$ additionally controls the magnitude of the log-amplitude variance in anisotropic random media. Eqs (14) and (15) for the variance of the log-amplitude complement the corresponding equations for the variance of the phase fluctuations (see eqs 20 and 29 in Samuelides

1998). Fig. 2 shows the log-amplitude variance according to eq. (14) as a function of the wave parameter for a fixed value of $ka_\perp$, but with varying parameter γ.

From eqs (14) and (15) we can roughly estimate the range of applicability of eq. (10). For the isotropic case, i.e. $\gamma = 1$, inequality (5) must be satisfied. For the anisotropic case ($\gamma \neq 1$), it is natural to assume that inequality (5) extends to

$$\sigma_n^2 \frac{a_{||}}{a_\perp}(ka_\perp)^2 \frac{L}{a_\perp} < 1. \tag{16}$$

Consequently, if $\gamma < 1$, the log-amplitude variance (10) can be applied for larger travel distances compared with the isotropic case. The opposite is true if $\gamma > 1$. Then, one should observe stronger wavefield fluctuations as compared with the isotropic case. This is in agreement with the calculations of Kon (1994) and Beran & McCoy (1974). Note that relation (16), in fact, does not depend on the transverse correlation length $a_\perp$ and thus the validity range is formally the same as in eq. (5) provided that the correlation length a is replaced by the correlation length in the direction of wave propagation $a_{||}$. Although the wave apparently interacts with the transverse correlation scale, the strength of the log-amplitude fluctuations is controlled by the longitudinal correlation scale $a_{||}$. There is an additional restriction for the applicability of eq. (10), which results from the fact that backscattered waves are neglected within the Rytov approximation in 2-D and 3-D random media. It can be formulated as

$$\begin{cases} ka_\perp\gamma > 1 \text{ if } & \gamma < 1 \\ ka_\perp > 1 \text{ if } & \gamma > 1 \end{cases} \tag{17}$$

and is analogous to the condition $ka > 1$ in the isotropic case. The meaning of this constraint is also discussed in Section 6. In conclusion, eqs (16) and (17) define the validity range of eq. (10).

With increasing travel distances the wavefield fluctuations also increase. Once the strong wavefield fluctuation regime (the quantity $\sigma_n^2(ka)^2 L/a$ is comparable to or larger than unity) is reached, it is well known that the normalized variance of the intensity fluctuations m^2 (the so-called scintillation index) saturates, i.e. $m^2 \to 1$ if $\sigma_n^2(ka)^2 L/a = O(1)$ (Rytov *et al.* 1989). It is easy to show that the variance of the intensity fluctuations and that of the log-amplitude fluctuations are related via $m^2 = \exp(4\,\sigma_\chi^2) - 1$ (Shapiro & Kneib 1993). Consequently, for $m^2 \to 1$ the log-amplitude variance tends to the constant $\frac{1}{4}\ln(2) = 0.173$. This result is true if the incident wave has unit intensity and backscattering can be neglected and is a manifestation of energy conservation within the parabolic approximation method (e.g. Rytov *et al.* 1989). That is to say, the very same saturation constant must be obtained regardless of the correlation properties of the medium:

$$^{\text{aniso}}\sigma_\chi^2 = {}^{\text{iso}}\sigma_\chi^2 = 0.173, \tag{18}$$

where $^{\text{iso}}\sigma_\chi^2$ and $^{\text{aniso}}\sigma_\chi^2$ denote the log-amplitude variance in isotropic and anisotropic random media, respectively. On the other hand, from eqs (7) and (14) it becomes clear that the log-amplitude variance in the weak fluctuation regime depends on the correlation properties. In fact, comparing eqs (7) and (14) we can deduce

$$^{\text{aniso}}\sigma_\chi^2 \approx \gamma\, {}^{\text{iso}}\sigma_\chi^2. \tag{19}$$

It is interesting to infer the behaviour of the log-amplitude variance in the region before the saturation limit is reached and where the discrepancy between eqs (18) and (19) is resolved. From the general behaviour of the scintillation index it is known that there is a maximum of m^2 before it reaches unit value (Uscinski 1975). The location and the magnitude of this maximum value depend on the correlation properties of the medium (for example, the maximum is more pronounced in a Gaussian correlated medium than in an exponentially correlated one). Therefore, we can also expect a different maximum value, $^{\max}\sigma_\chi^2$, for different values of γ in anisotropic random media. In fact, from our numerical experiments (to be discussed in the next section) we find that

$$^{\max}\sigma_\chi^2 \propto \frac{1}{\gamma}. \tag{20}$$

This means that if $\gamma < 1$ we can observe a more pronounced maximum of σ_χ^2 than in isotropic random media. Note that in the case of $\gamma \ll 1$ our consideration is not valid because the Rytov approximation for σ_χ^2 in 3-D does not take into account backscattered waves. On the other hand, if $\gamma \gg 1$, the maximum value of σ_χ^2 is much smaller than that of the isotropic case and occurs at shorter propagation distances. However, in such a case the successive increase of the scattering angles with propagation distance violates the assumption of forward scattering and our results are no longer valid (see also the introduction).

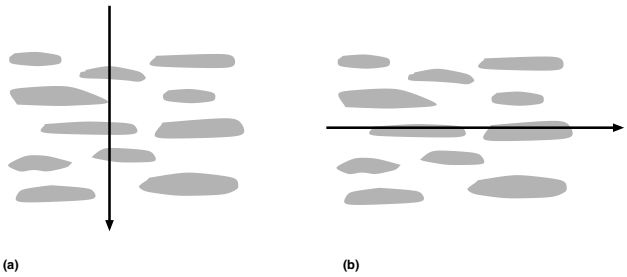

Figure 1. Geometry for wave propagation in anisotropic random media. Two cases are of particular interest: (a) the main direction of wave propagation parallel to the short axis of the inhomogeneities and (b) the main direction of wave propagation parallel to the long axis of the inhomogeneities. For both cases we present explicit results of the log-amplitude variance if the inhomogeneities are Gaussian correlated.

5 NUMERICAL VERIFICATION

In order to verify eqs (14) and (15), we perform finite-difference simulations of wave propagation in 2-D random media. Similar numerical experiments have been performed by Shapiro & Kneib (1993) and Müller *et al.* (2002) for isotropic random media. Results of numerical simulations of seismic waves in anisotropic random media are also presented in Ikelle *et al.* (1993). In this study, a plane wave (a Ricker wavelet with a dominant frequency of 43 Hz) propagating in the homogeneous reference medium ($c_0 = 3000$ m s^{-1} and $n(\mathbf{r})$=0) impinges on a slab of an anisotropic random medium realization, where the inhomogeneities are Gaussian correlated (with a standard deviation of 5 per cent and correlation scales specified below). Note that the random process n corresponds to the fluctuations of the squared slowness. However, in the numerical experiment it is more convenient to work directly with velocity fluctuations. For weak fluctuations ($\sigma_n^2 \lesssim 0.15$) we can use $\sigma_n^2 \approx \sigma_v^2$ without incurring an error. The long (short) axis of the inhomogeneities is perpendicular to the direction of wave propagation (Fig. 1). Inside the random medium the initially plane wavefield becomes distorted and is recorded by 20 receiver lines perpendicular to the main propagation direction. Each receiver line consists of 150 geophones separated by the distance of the horizontal correlation length.

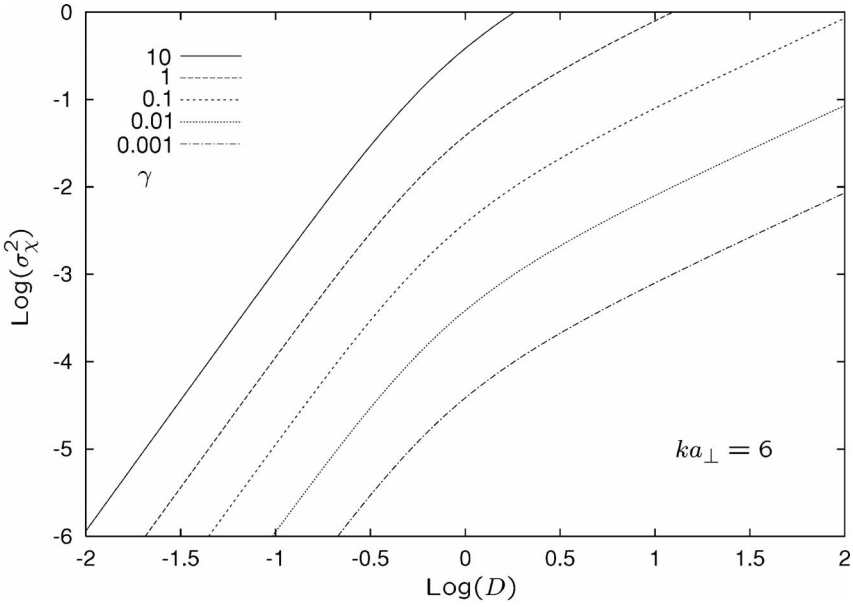

Figure 2. The normalized log-amplitude variance (14) as a function of the wave parameter for varying γ and fixed $ka_\perp$. Compared with the isotropic case ($\gamma = 1$), σ_χ^2 is increased for $\gamma > 1$ and decreased for $\gamma < 1$. The characteristic dependence on the wave parameter D is the same for all γ. For $D \ll 1$, $\sigma_\chi^2 \propto D^3$, whereas for $D \gg 1$, $\sigma_\chi^2 \propto D$ (see the discussion in Rytov *et al.* 1989).

The log-amplitude variance is extracted from the synthetic seismograms in the following way.

(1) A box-car window is applied around the primary arrivals. The window length increases with increasing travel distance (this is in accordance with the results of Müller *et al.* (2002), where it is shown that the broadening of the primaries is approximately proportional to $\sqrt{L}$). We note that in a strict sense it is not adequate to test a theory for harmonic wavefields (eq. 2) using windowed seismograms. However, in a wavefield fluctuation regime, where forward scattering prevails, the use of windowed seismograms is justified because most of the wavefield energy is localized in the vicinity of the first arrivals. One crucial parameter is the window length applied in order to extract the primaries (see Shapiro & Kneib 1993, for a more detailed discussion on this issue).

(2) The amplitude spectrum of the windowed seismograms is computed.

(3) We take the logarithm of the amplitude spectrum $A(\omega)$ and subtract the logarithm of the amplitude spectrum of the incident pulse $A_0(\omega)$. Evaluating this function at the dominant frequency ω_0 yields the quantity $\chi(\omega_0)$ (eq. 3).

(4) We average the log-amplitude χ over all geophones along one receiver line in order to obtain the log-amplitude variance (using eq. 4). We note that the theory given above predicts the ensemble-averaged log-amplitude variance. However, in our simulations we derive σ_n^2 from wavefield realizations recorded in one realization of the random medium. In order to derive the ensemble-averaged σ_n^2 we make implicitly use of the ergodicity hypothesis: spatial averaging of a sufficient large number of statistically independent measurements within one realization should be an estimate of the ensemble-averaged value. In particular, this assumption is justified if the wavefield realizations are measured at locations which are separated by a distance that exceeds the coherence radius of the wavefield. In our simulations the geophones along one receiver line are separated by more than one correlation length ($a_\perp$) so that statistically independent measurements are obtained.

Repeating steps (1)–(4) for all receiver lines yields the desired log-amplitude variance as a function of travel distance.

The numerical results are displayed in Fig. 3. To emphasize the differences with the isotropic case, we performed a reference experiment (i.e. $a_\parallel = a_\perp = 45$ m) for which the evaluated log-amplitude variance is shown in the upper plot. Up to travel distances of 500 m the numerical results (illustrated by crosses) closely follow the theoretical prediction (the solid line), i.e. eq. (15) with $\gamma = 1$. For travel distances larger than 500 m the weak fluctuation regime is no longer valid (restriction (16) yields for $L = 500$ m a value of $\sigma_\chi^2 \approx 0.5$), and the σ_χ^2 estimate for the strong fluctuation regime roughly applies (the constant 0.25 ln (2) is indicated by the dotted line). That the numerically determined values exceed this constant value is caused by several reasons. First, there is a transition from weak to strong wavefield fluctuations, where the log-amplitude variance is maximal and exceeds the saturation limit. The maximum value depends on the correlation properties of the random medium (see the last paragraph in Section 4). In our experiments, this transition takes place for travel distances around 600 m. Secondly, for travel distances larger than ≈700 m we expect that σ_χ^2 approaches the saturation limit. However, in the regime of stronger wavefield fluctuations it is not possible to window the data without introducing a bias in the amplitude spectra. Moreover, in such a regime it is no longer possible to distinguish between primary waves and later arrivals. Generally, we observed that for stronger wavefield fluctuations our procedure of extracting σ_χ^2 from the primary wavefield becomes less accurate. We note that an alternative method would be the phase screen method as demonstrated by Hoshiba (2000). In fact, Hoshiba (2000) modelled the transition from weak to strong wavefield fluctuations and was able to reproduce the saturation limit very well.

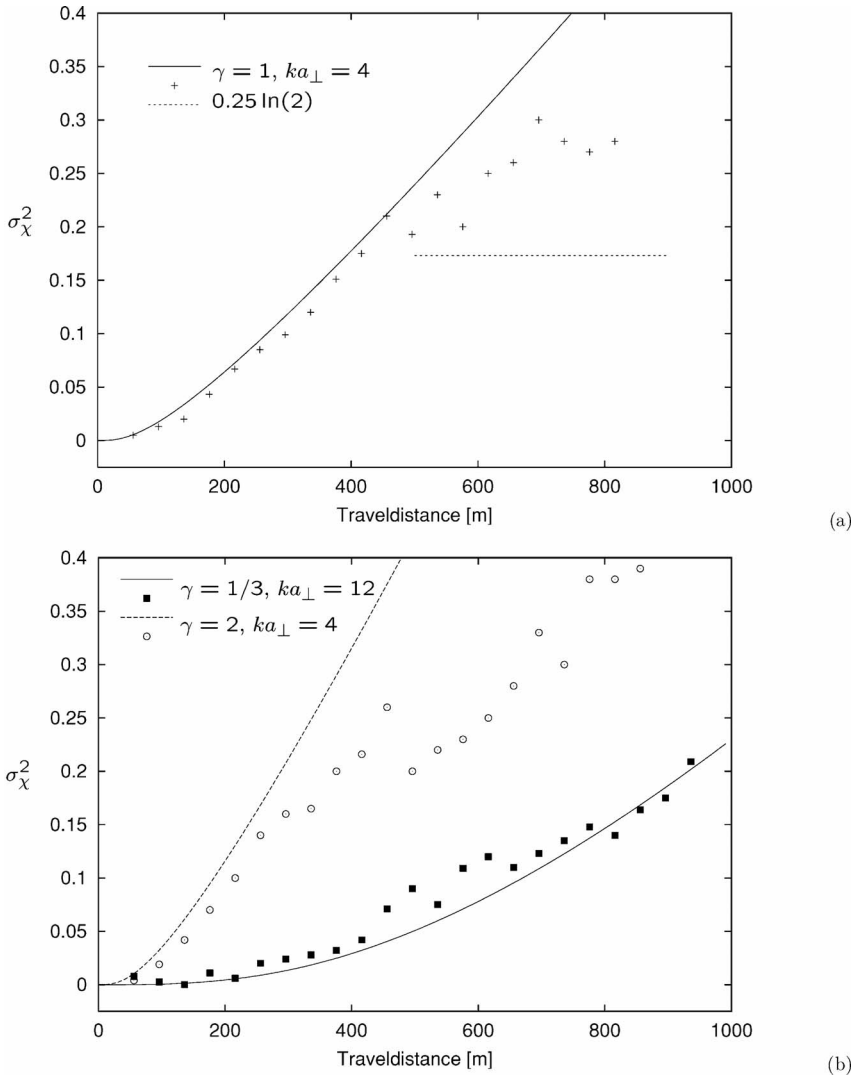

Figure 3. The log-amplitude variance as a function of the travel distance. The results for a reference experiment in isotropic random media is shown in (a) (the solid line denotes σ_χ^2 according to eq. (15), the crosses denote the numerically determined values). In (b) the results for σ_χ^2 in anisotropic random media for two values of $\gamma = a_{||}/a_\perp$ are presented (the lines correspond to formula (15), the diamonds and rectangles denote the corresponding numerical results). Apart from the correlation lengths, the medium parameters are in all experiments the same: $c_0 = 3000$ m s^{-1}, $\sigma_v = 0.05$ and the value of k is derived from the dominant frequency of 43 Hz.

The numerical results for anisotropic media are displayed in the lower plot of Fig. 3. In a further experiment we choose $a_{||} = 90$ m and $a_\perp = 45$ m so that $\gamma = 2$ and as predicted by eq. (15) the σ_χ^2 values grow more rapidly with travel distance (the dotted line and circles, respectively). It can also be observed that the range of the weak fluctuation regime is restricted by smaller travel distances compared with the isotropic case (in agreement with restriction (16)). The strong fluctuation regime apparently begins at $L \approx 300$ m, however, there is no indication of a saturation of the log-amplitude variance, but a staircase-like pattern is formed. This is probably caused by two mechanisms. First, as in the isotropic case the numerical evaluation of σ_χ^2 becomes less accurate when the wavefield fluctuations are strong. Secondly, as mentioned in the introduction, for wave propagation along the longer axis of the inhomogeneities it is known that the scattering angles are no longer small and thus there is a considerable amount of backscattering, which is neglected in the consideration of the strong-fluctuation-regime estimate of σ_χ^2 (see also the last paragraph of Section 4). Further numerical considerations (results are not shown) indicate that for even larger values of γ the presented formulae cannot be applied (in agreement with restriction (16)). A common travel distance gather for $L = 500$ m is displayed in Fig. 5 (bottom, see later) showing a strongly distorted primary wave, which is a qualitative indication for these strong wavefield fluctuations.

The numerical results for wave propagation along the short axis of the inhomogeneities is also displayed in the lower plot of Fig. 3. Here, we choose $a_{||} = 45$ m and $a_\perp = 135$ m so that $\gamma = \frac{1}{3}$. The numerically determined σ_χ^2 values (the filled squares) fit the theoretical result given by eq. (15) (the solid line) quite well over the whole travel distance interval under consideration ($L = -1000$ m). This is again in agreement with restriction (16), which predicts an increased range of validity of the Rytov approximation for wave propagation along the shorter axis of the inhomogeneities ($\gamma < 1$). In this case, the regime of strong wavefield fluctuations is beyond

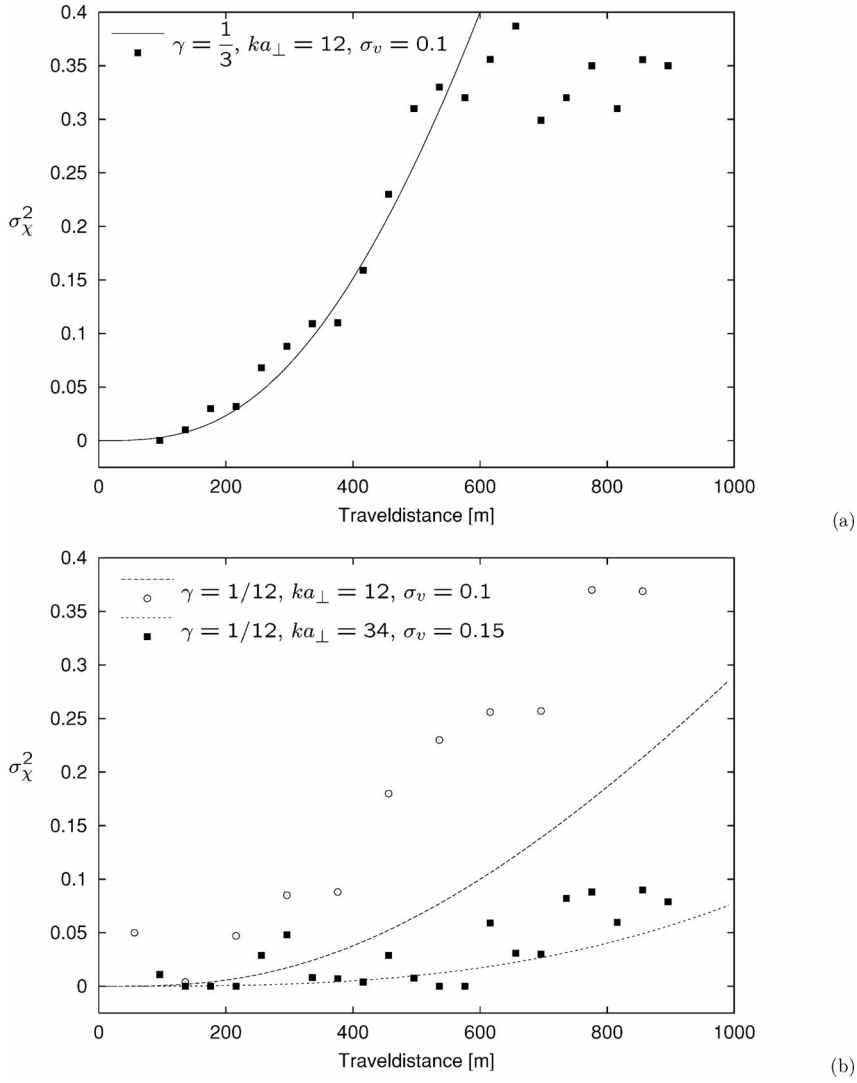

Figure 4. The log-amplitude variance as a function of travel distance determined from experiments, where the limits of applicability are reached (see the main text for an explanation). In (a) and (b) we used $c_0 = 3000$ m s^{-1} and a dominant frequency of 43 Hz. The strength of the perturbations and the ratio of spatial anisotropy are indicated in the legend.

the domain of our numerical simulation. That the numerical estimates of σ_χ^2 fluctuate slightly more strongly around the theoretical curve compared with the isotropic case is a purely numerical effect because less statistically independent measurements are made (i.e. the distance between two geophones is less than the horizontal correlation length). Averaging the results of more experiments involving different realizations of the random medium would give a better agreement with the theory.

In order to exemplify the increased range of applicability of the Rytov approximation for σ_χ^2 (and to assess its limitations) we perform further experiments. First, we repeat the last experiment with $\gamma = \frac{1}{3}$, however, for a medium with stronger velocity fluctuations ($\sigma_v = 10$ per cent). The extracted log-amplitude variances are shown in Fig. 4(a) by the black squares. The theoretical prediction is shown by the solid curve, which gives a good approximation for the numerically determined values up to $L \approx 500$ m. For larger travel distances we observe a deviation from the theoretical prediction of the log-amplitude variances, indicating the beginning of the strong fluctuation regime. Comparing this result with that of the corresponding isotropic case, where $\sigma_v = 5$ per cent (displayed in Fig. 3a), we observe the same range of travel distances, where eq. (15) gives a good approximation in spite of the fact that σ_v is twice as large. This is in agreement with eq. (16): in anisotropic random media with $\gamma < 1$ we may increase the medium contrasts without violating the range of applicability. There is, however, a significant difference for the two experiments regarding the magnitude of the log-amplitude variances. This difference is still visible when approaching the saturation limit (though within our numerical procedure we are not able to resolve the saturation limit properly). It can be clearly observed that within the transition from weak to strong wavefield fluctuations (i.e. for travel distances between 500 and 800 m in Fig. 4a), the magnitude of σ_χ^2 is increased significantly compared with the isotropic case. This increase can be qualitatively explained using proportionality (20).

Decreasing γ increases the range of applicability of the formulae for σ_χ^2. However, arbitrary small values of γ are only admitted if, at the same time, conditions (16) and (17) are satisfied. This is demonstrated by the following examples. Choosing $\sigma_v = 10$ per cent,

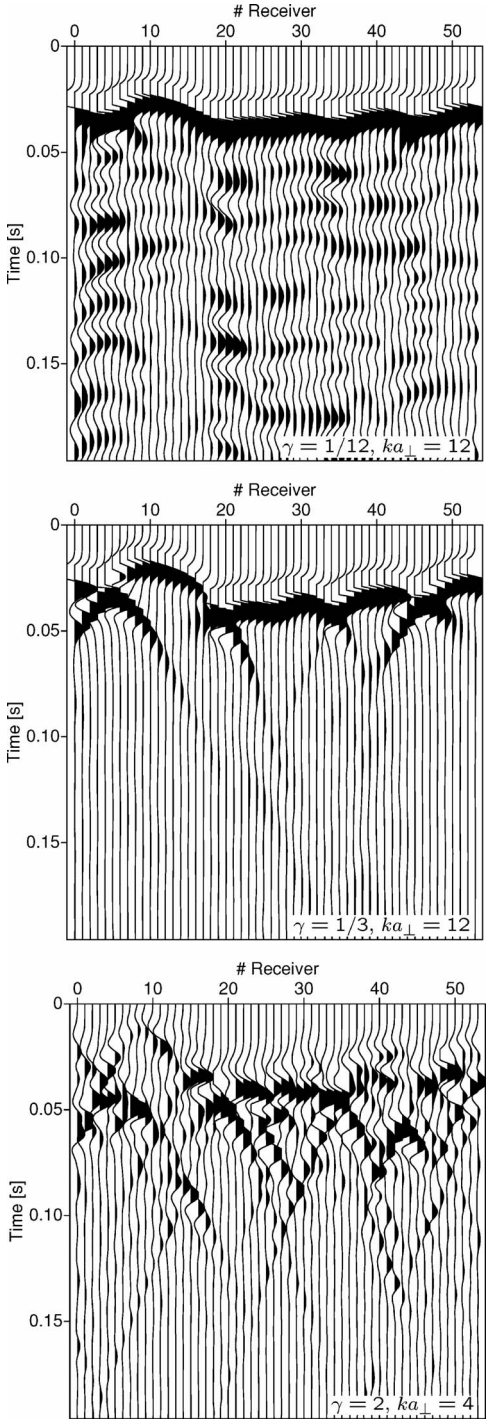

Figure 5. Simulated common travel distance gather ($L = 500$ m) in anisotropic random media ($c_0 = 3000$ m s^{-1}) with varying γ (indicated at the lower right-hand corner of each plot) and fixed perturbation strength ($\sigma_v = 0.1$). Top: condition (17) is violated and the random diffractions and refractions are superimposed with spatially coherent 'multiple reflections'. Middle: conditions (16) and (17) are satisfied and the formulae for the σ_χ^2 work well. Bottom: condition (16) is violated and the beginning of the strong fluctuation regime becomes visible through the decomposition of the clearly distinguishable ballistic wave (the primary wave) into random fluctuations.

$a_\perp = 135$ m and $a_{||} = 11.25$ m (we then have $\gamma = \frac{1}{12}$), the resulting values of σ_χ^2 are displayed by the unfilled circles in Fig. 4(b). The theoretical prediction is plotted as a dashed line. Obviously, there is no longer agreement between theory and experiment. The reason for this discrepancy is the violation of condition (17) (now $ka_{||} \lesssim 1$). In such a model we expect a significant contribution to the attenuation due to backscattering from quasi-1-D inhomogeneities and a reduced contribution due to random diffractions and refractions (see the discussion in Section 6). The change in the significance of the physical mechanism that causes attenuation also becomes visible in the spatial energy redistribution of waves propagating in an inhomogeneous medium. The uppermost plot in Fig. 5 displays a common travel distance gather for the experiment under consideration. Apart from random diffractions (visible through fluctuating amplitudes for a fixed time), the wavefield behind the primary wave is composed of 'multiples' that are similar in shape (but reduced in amplitude) compared with the primary wave. A quite different picture gives the common travel distance gather for a reference experiment, where condition (17) is satisfied (middle plot in Fig. 5). Here the wavefield fluctuations are concentrated in the vicinity of the wave front which is, however, more distorted than that of the previous experiment. Moreover, the randomly distributed diffractions and refractions are clearly visible. In such a situation the presented formulae for σ_χ^2 can still be applied. This is also demonstrated in an experiment with $\sigma_v = 15$ per cent, where condition (17) is met ($a_\perp = 360$ m and $a_{||} = 30$ m), however, due to the strong fluctuations we reach the limit of condition (16) (now $\sigma_v^2 (ka_{||})^2 L/a_{||} \gtrsim 1$ for $L \gtrsim 200$ m). Consequently, the numerically determined values of σ_χ^2 slightly exceed the theoretical prediction (see the squares and the dotted line in Fig. 4b and the corresponding seismogram section in Fig. 5).

6 DISCUSSION

That the log-amplitude variance calculated in the Rytov approximation serves as an estimate of attenuation due to diffraction and refraction at randomly distributed velocity inhomogeneities (in connection with eq. 6) becomes evident once more when we consider the limit $a_\perp \to \infty$ (while $a_{||}$ remains finite), which corresponds to a purely layered random medium. In such a case, the log-amplitude variance vanishes and resembles the fact that in 1-D random media no diffraction effects nor random foci due to refraction (nor intersecting 'rays') occur. Thus, in addition to the limits of applicability of the Rytov approximation to estimate the amount of scattering attenuation (weak wavefield fluctuations), there is a further constraint in anisotropic random media: for a certain ratio of anisotropy ($\gamma \ll 1$) and for wavelengths that exceed the correlation distance in the direction of wave propagation those diffraction and refraction effects, which cause amplitude fluctuations along the direction perpendicular to the direction of propagation, play a minor role. Then the attenuation of primary waves is mainly caused by backscattering, and primary amplitudes are given by constructive interference of parts of the wavefield that are multiply reflected and refracted (transmitted) at quasi-1-D impedance contrasts. This resembles the physics of scattering attenuation in 1-D random media, which is maximal for $ka = 1$ and is larger than in 2-D and 3-D random media if $ka < 1$ (because of the universal Rayleigh scattering frequency dependence $\alpha \propto \omega^{d+1}$, where d denotes the spatial dimension). That is why the description of scattering attenuation of primary waves within the Rytov theory in 2-D and 3-D anisotropic random media is principally limited by the neglect of backscattering (constraint 17).

It is interesting to relate the above description of scattering attenuation of primaries in anisotropic random media to existing full-frequency-range-valid approximations, which have been obtained for 3-D isotropic random media, on the one hand, and 1-D random media, on the other hand. For 3-D (and also 2-D) isotropic random media Müller *et al.* (2002) derived within the weak scattering regime a solution for the scattering coefficient α, which is attached to the most probable primary pulse (note that in 3-D there are a multitude of possible realizations of primary pulses). This dynamic solution of α has been obtained by combining the Rytov approximation (compare with eq. 7 for the log-amplitude variance) with another perturbation approximation that partially takes into account backscattering. In contrast to this, the present results are only based on the Rytov approximation, which completely neglects backscattered waves and thus restricts the validity of α with respect to the frequency range as discussed in the previous paragraph. For 1-D random media (Shapiro & Hubral 1999) obtained approximations of the scattering attenuation coefficient within the so-called *generalized O'Doherty–Anstey* (ODA) approach. This is formally equivalent to the second-order Rytov approximation for 1-D random media, which has the remarkable property of accounting for backscattered waves. A general description of scattering attenuation in 3-D anisotropic random media, which reduces in the layered-media limit to the results of the ODA approach, has not been reported so far. However, we think that the present results are a first step towards this goal.

The quantification of seismic scattering attenuation along with estimates of the correlation scales and the spatial orientation of subsurface heterogeneities in the crust and mantle may contribute to the understanding of large-scale geoprocesses. Incorrect estimates of scattering attenuation can lead to serious misinterpretations of rock properties and structural images. If there is evidence for the presence of anisotropic inhomogeneities (which in many geological settings is the case, see the introduction), this information must be taken into account in the calculation and interpretation of scattering attenuation. The above results can also provide a useful correction to the scattering attenuation estimates obtained from seismo-stratigraphic considerations when additionally the finite lateral extent of geological structures is taken into account. The combination of the scattering attenuation descriptions for 1-D and 3-D random media is the topic of a forthcoming paper.

In Müller & Shapiro (2001) scattering attenuation estimates for the German KTB area were obtained with the aid of statistical estimates of velocity inhomogeneities deduced from the well-log data. With the assumption of statistically isotropic inhomogeneities, they explained a large amount of the 'measured' attenuation (extracted from the seismic data of the accompanying VSP experiment) in terms of scattering. A previously reported hypothesis (Lüschen *et al.* 1993) assumes that seismic reflectivity is mainly related to scattering at hydraulically active fracture zones. We hypothesize that such fracture systems can effectively act like an anisotropic random medium, where the largest correlation scale is associated with the average direction of the fractures and cracks. Moreover, to assume spatial anisotropy is necessary because in fracture systems there is a preferred orientation of cracks that is associated with the orientation of major faults. Taking into account the steeply inclined major faults in the KTB region (for depths up to 10 km the dip angle is typically 30°–70°, see e.g. Harjes *et al.* 1997), it is reasonable to assume that the seismic waves in the VSP experiment travelled to some extent parallel to the cracks and thus along the long axis of the anisotropic random medium such that the case $\gamma > 1$ applies. For the evaluation of scattering attenuation this has an important consequence. As shown above, for $\gamma > 1$ larger scattering attenuation estimates are obtained compared with the isotropic case. Taking into account this fact, we speculate that the amount of scattering attenuation at the KTB area can be even larger than that evaluated in Müller & Shapiro (2001).

7 CONCLUSIONS

In conclusion, we derived simple explicit results for the log-amplitude variance in anisotropic random media based on the Rytov approximation. Assuming Gaussian correlated inhomogeneities we obtain explicit results, which are confirmed by numerical simulations. For wave propagation along the large axis of inhomogeneities, the Rytov approximation is not the best choice because of its limited range of validity. The opposite is true for wave propagation along the short axis of the inhomogeneities. Then the Rytov approximation for the log-amplitude variance (and also the variance of the phase fluctuations) has a wider range of applicability compared with the isotropic case. Furthermore, we formulate conditions that define the range of applicability of the presented formulae. We discussed the use of the log-amplitude variance as an estimate of scattering attenuation in anisotropic random media. Caution is required in the case $\gamma \ll 1$, because the attenuation of seismic primaries due to random diffraction and refraction in the presented approximation may then be small compared with the attenuation that is caused due to backscattering. It remains to be tested whether a combination of 1-D Q-estimates that account for backscattering (such as obtained from the ODA approach) and the presented results for Q in 3-D anisotropic random media is more adequate for modelling Q-measurements in layered structures with a finite lateral extent.

ACKNOWLEDGMENTS

We appreciate the critical and constructive comments of two anonymous reviewers, which greatly improved the quality of the manuscript. This work was kindly supported by the sponsors of the *Wave Inversion Technology (WIT) Consortium* and by the Deutsche Forschungsgemeinschaft (contracts SH55/2-2 and MU1725/1-1).

REFERENCES

Beran, M.J. & McCoy, J.J., 1974. Propagation through an anisotropic random medium, *J. Math. Phys.,* **15,** 1901–1912.

Dashen, R., 1979. Path integrals for waves in random media, *J. Math. Phys.,* **20,** 894–920.

Harjes, H.-P. *et al.,* 1997. Origin and nature of crustal reflections: results from integrated seismic measurements at the KTB superdeep drill hole, *J. geophys. Res.,* **102,** 18 267–18 288.

Hoshiba, M., 2000. Large fluctuations of wave amplitude produced by small fluctuations of velocity structures, *Phys. Earth planet. Interiors,* **120,** 201–217

Ikelle, L.T., Yung, S.K. & Daube, F., 1993. 2-D random media with ellipsoidal autocorrelation functions, *Geophysics,* **58,** 1359–1371.

Ishimaru, A., 1978. *Wave Propagation and Scattering in Random Media,* Academic, New York.

Klimeš, L., 2002. Correlation functions of random media, *Pure appl. Geophys.,* **159,** 1811–1831.

Knollman, G.C., 1964. Wave propagation in a medium with random, spheroidal inhomogeneities, *J. acoust. Soc. Am.,* **36,** 681–688.

Komissarov, V.M., 1964. Amplitude and phase fluctuations and their correlation in the propagation of waves in a medium with random, statistically anisotropic inhomogeneities, *Sov. Phys.-Acoustics,* **10,** 143–152.

Kon, A.I., 1994. Qualitative theory of amplitude and phase fluctuations in a medium with anisotropic turbulent irregularities, *Waves Random Media,* **4,** 297–306.

Lüschen, E., Sobolev, S., Werner, U., Söllner, W., Fuchs, K., Gurevich, B. & Hubral, P., 1993. Fluid reservoir (?) beneath the KTB drillbit indicated by seismic shear wave observations, *Geophys. Res. Lett.,* **20,** 923–926.

Müller, T.M. & Shapiro, S.A., 2001. Seismic scattering attenuation estimates for the German KTB area derived from well-log statistics, *Geophys. Res. Lett.,* **28,** 3761–3764.

Müller, T.M., Shapiro, S.A. & Sick, C.M.A., 2002. Most probable ballistic waves in random media: a weak-fluctuation approximation and numerical results, *Waves Random Media,* **12,** 223–245.

Ryberg, T., Fuchs, K., Egorkin, A.V. & Solodilov, L., 1995. Observation of high-frequency teleseismic P-N on the long-range quartz profile across Northern Eurasia, *J. geophys. Res.,* **100,** 18 151–18 163.

Rytov, S.M., Kravtsov, Yu.A. & Tatarskii, V.I., 1989. Principles of Statistical Radiophysics, Vol. 4: *Wave Propagation Through Random Media,* Springer, Berlin.

Samuelides, Y., 1998. *Velocity shift using the Rytov approximation, J. acoust. Soc. Am.,* **105,** 2596–2603.

Sato, H. & Fehler, M., 1998. *Wave Propagation and Scattering in the Heterogeneous Earth,* AIP Press, Springer, New York.

Shapiro, S.A. & Kneib, G., 1993. Seismic attenuation by scattering: theory and numerical results, *Geophys. J. Int.,* **114,** 373–391.

Shapiro, S.A. & Hubral, P., 1999. *Elastic Waves in Random Media,* Springer, Heidelberg.

Tittgemeyer, M., Wenzel, F., Ryberg, T. & Fuchs, K., 1999. Scales of heterogeneities in the continental crust and upper-mantle, *Pure appl. Geophys.,* **156,** 29–52.

Tripathi, J.N., 2001. Small-scale structure of lithosphere–asthenosphere beneath Gauribidanur seismic array deduced from amplitude and phase fluctuations, *J. Geodyn.,* **31,** 411–428.

Uscinski, B.J., 1975. *The Elements of Wave Propagation in Random Media,* McGraw-Hill, New York.

Wagner, G.S., 1998. Local wave propagation near the San Jacinto fault zone, Southern California: observations from a three-component seismic array, *J. geophys. Res.*, **103,** 7231–7246.

Wu, R.-S. & Flatté, S.M., 1990. Transmission fluctuations across an array and heterogeneities in the crust and upper mantle, *Pure appl. Geophys.,* **132,** 175–196.

Wu, R.-S., Xu, Z. & Li, X.-P., 1994. Heterogeneity spectrum and scale-anisotropy in the upper crust revealed by the German continental deep-drilling (KTB) holes, *Geophys. Res. Lett.,* **21,** 911–914.